

Insight into the Jet Emission Properties from Long-Term Monitoring of the TeV Blazar PG 1553+113

E. Prandini,^{a,*} T. Hovatta,^b G. Silvestri^a and A. Stamerra^c for the MAGIC collaboration

^a*Università di Padova and INFN, I-35131 Padova, Italy*

^b*Finnish Center for Astronomy with ESO (FINCA), University of Turku, FI-20014 Turku, Finland, Aalto University Metsahovi Radio Observatory, Metsahovintie 114, FI02540 Kylmala, Finland, and Aalto University Department of Electronics and Nanoengineering, PL 15500, FI-00076 Aalto, Finland*

^c*National Institute for Astrophysics (INAF), I-00136 Rome, Italy*

E-mail: elisa.prandini@unipd.it

PG 1553+113 is a distant TeV blazar known for its 2.2-year periodic gamma-ray signal detected with *Fermi*-LAT. We present results from a decade-long, multiwavelength monitoring campaign of this source. Our analysis confirms the periodicity in gamma-ray and optical bands; however, no significant periodicity is found at TeV and X-ray energies, based on observations with MAGIC and Swift-XRT, respectively. These findings, combined with a study of variability on different timescales, support a multi-zone emission scenario, as further corroborated by recent IXPE observations. We test a two-zone, synchrotron self-Compton model on 2019 multi-frequency flare data. The long- and short-term variability, along with inter-band correlations from the monitoring, serve as key inputs to constrain the model, reducing the large degrees of freedom. Based on this approach, we propose a set of parameters that effectively describe the PG 1553+113 emitting region responsible for the observed radiation.

39th International Cosmic Ray Conference (ICRC2025)
15–24 July 2025
Geneva, Switzerland



ICRC 2025

The Astroparticle Physics Conference
Geneva July 15-24, 2025

*Speaker

1. PG 1553+113: a periodic γ -ray blazar

Variability across a broad range of timescales is a hallmark of active galactic nuclei (AGN) [1], and particularly prominent in blazars, a subclass dominated by jet emission from a relativistic outflow closely aligned with our line of sight. This geometry leads to Doppler-boosted, highly variable, non-thermal emission extending from radio to TeV energies, with a spectral energy distribution (SED) typically showing two humps: synchrotron emission peaking in the IR to X-rays, and a high-energy component from inverse-Compton or hadronic processes [2]. Blazars are classified as flat-spectrum radio quasars (FSRQs) or BL Lacertae objects (BL Lacs) based on the optical emission line strength, and further subtyped by the synchrotron peak frequency into low, intermediate, and high synchrotron-peaked (LSP, ISP, HSP) sources [3]. Variability amplitudes can reach two orders of magnitude and occur on timescales from minutes to years [4]. While short-term variability is often attributed to turbulent or shock-driven jet activity, long-term patterns remain less understood and may trace deeper physical or geometric processes in the jet or central engine [5, 6].

The HBL object PG 1553+113 is one of the most prominent TeV blazars. Absorption features in its UV spectrum suggest a redshift of $z \sim 0.433$ [7], making it a valuable probe of extragalactic background light (EBL) attenuation [8, 9]. Despite significant gamma-ray absorption above 250 GeV, it has been detected by all major IACTs [10, 11].

A ~ 2.2 year periodic modulation has been detected in its *Fermi*-LAT gamma-ray lightcurve at $E > 100$ MeV and $E > 1$ GeV, with $< 1\%$ false-alarm probability over 3.5 cycles [12], and confirmed by several studies [13–15]. Optical lightcurves exhibit a matching 2.06 ± 0.05 year modulation over 4.5 cycles, tightly correlated with gamma-ray variability. These findings make PG 1553+113 one of the strongest QPO candidates in the blazar population. Periodic modulation in blazars may arise from different mechanisms. Geometric scenarios include jet precession, helical motion, or changes in viewing angle [16, 17], potentially causing achromatic variability through Doppler boosting [18]. Alternatively, jet modulation may stem from accretion disk instabilities [19, 20], or from binary SMBH interactions, with the secondary inducing perturbations near periastron [21, 22]. VLBA monitoring between 2015 and 2017 revealed changes in the jet position angle [23], suggesting a possible geometric contribution to the variability. However, no clear temporal match with the gamma-ray/optical QPO was found, indicating additional mechanisms may be involved. Polarimetric studies during flaring episodes also suggest a mix of stochastic and deterministic components [24].

Flaring on weekly timescales in PG 1553+113 has been studied extensively [10, 25], helping constrain intrinsic emission models and test phenomena like Lorentz invariance violation [26]. Nonetheless, the physical origin of mid and long-term periodicity remains unsettled, requiring rigorous statistical analysis and multiwavelength correlation. To investigate these processes, the MAGIC collaboration initiated a multi-year MWL campaign in 2015, involving radio, IR, optical, UV, X-ray, and gamma-ray instruments. In this contribution, we present the results of this effort, aiming to characterize the broadband variability of PG 1553+113, and assess the nature of its periodic emission based on data collected from 2007 to 2017. These findings were recently published in [27]. As a next step in our analysis, we discuss the modeling of the 2019 spectral energy distribution (SED) during both flaring state and lower activity (MAGIC Coll. paper in preparation).

2. Multiwavelength observations of PG 1553+113

In [27], we analysed the multiwavelength (MWL) behaviour of PG 1553+113 over the period 2007–2017, using MAGIC observations complemented by data from radio to very high-energy (VHE) gamma rays. The decadal lightcurve of PG 1553+113 is illustrated in figure 1. The primary goal of the study was to investigate whether the ~ 2.2 -year periodicity detected in the GeV gamma-ray band by the *Fermi*-LAT [12] is also present in the MAGIC data, and to assess whether the MWL dataset can constrain the physical scenarios proposed to explain such periodicity.

To this end, we first characterised the variability in the VHE gamma-ray and X-ray bands. No evidence for intraday variability was found in either band. However, previous studies reported X-ray intraday variability in PG 1553+113, notably Raiteri et al. [24], who analysed long *XMM-Newton* exposures from 2015 and found flux changes on timescales of ~ 1 hour, implying a compact emission region with size $R \lesssim \delta \times 10^{14}$ cm. More recently, Dhiman et al. [28] confirmed intraday variability in the 0.3–10 keV band using *XMM-Newton* data from 2010–2018. Variability was detected in 16 out of 19 observations, with durations ranging from 21 to 140 ks and doubling timescales between 2 and 33 ks (~ 30 minutes to 9 hours). Due to the short duration of our individual pointings, our dataset lacked the temporal resolution necessary to probe such intranight variability. The X-ray data in our sample exhibit a mild harder-when-brighter trend, commonly observed in blazars, although typically on shorter timescales. This behaviour may indicate variability driven by the injection of fresh, high-energy electrons. A similar analysis applied to the MAGIC data yielded inconclusive results, likely due to the one-month time binning.

3. Variability patterns: evidence for a two zone emitting scenario

3.1 Periodicity search

A comprehensive multiwavelength (MWL) study of PG 1553+113 over the period 2007–2017 reveals valuable insights into the long-discussed periodic modulation observed in its emission. A folded lightcurve analysis, assuming a period of 798 days as first proposed in Ackermann et al. [12] and supported by further works [14, 15, 31], shows a coherent modulation pattern across multiple bands. The HE gamma-ray data from *Fermi*-LAT display a clear peak at phase ~ 0 and a minimum at phase 0.3–0.5, a trend echoed by the UV and optical lightcurves. The radio emission shows a phase shift consistent with delayed propagation effects, as also observed in discrete correlation function (DCF) studies [29]. Although sampling is sparser at higher energies, the X-ray and VHE gamma-ray folded lightcurves cover a broad range of phases, allowing qualitative comparison. All bands, including optical polarisation, appear to share a common minimum around phase 0.3–0.5, though a significant maximum is notably absent in the optical polarisation, X-ray, and VHE gamma-ray data.

A formal periodicity search using the Generalized Lomb-Scargle (GLS) periodogram, incorporating simulations of red-noise lightcurves to estimate statistical significance [30], confirms a strong periodic signal in the *Fermi*-LAT band, with a global p-value of 1.0×10^{-3} ($\sim 3.1\sigma$). The UV and radio bands show less significant, but still notable, consistency with the 798-day period, with global p-values of 10% and 3.4%, respectively, and local p-values at the literature period of 0.56% and 2%. In contrast, the optical band shows a broad, flat GLS peak between 800–1000 days

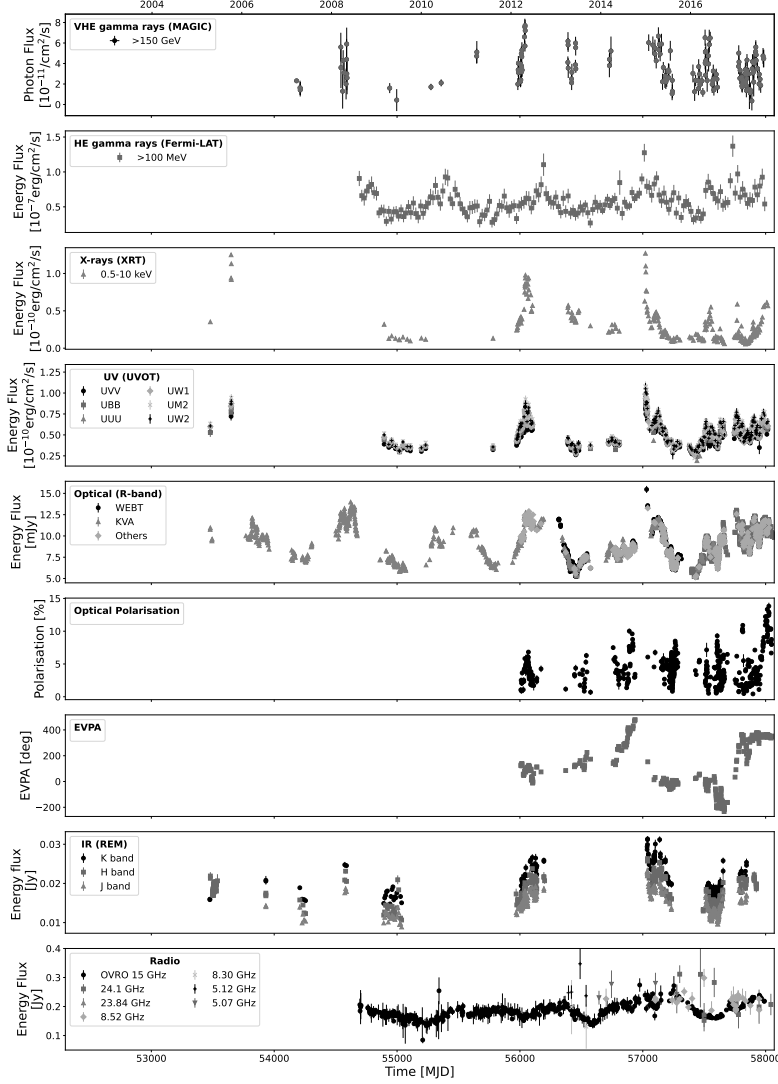


Figure 1: Multiwavelength, multi-epoch lightcurve of PG 1553+113. Adapted from [27].

and a poorly constrained period, with a global p-value of 47%. This is less significant than previous findings [31, 32], likely due to different sampling and method sensitivity. Additional analysis using the pipeline from Peñil et al. [15], including Lomb-Scargle and wavelet transforms, confirms the ~ 800 -day periodicity in the HE gamma-ray and suggests a possible - but not yet conclusive - signal in the optical band. No evidence of significant periodicity was found in the X-ray or VHE gamma-ray data, although a shorter periodicity has been suggested [33]. A summary of the derived periodicities, power spectral densities, and significance levels across all bands is provided in Table 1.

3.2 Intra-band correlation

Cross-band correlation studies spanning infrared (IR), optical, ultraviolet (UV), X-ray, high-energy (HE), and VHE gamma-ray bands revealed strong correlations within the IR/optical/UV

Table 1: Summary of periodicity search results across different energy bands. The power spectral density (PSD) index was extracted from the data. The peak period is the highest peak in the GLS periodogram. P-values are listed for the peak (local) and after correction for trial effects (global). Adapted from [27].

Band	PSD Index	Peak Period [d]	Peak Power	Local p-value	Global p-value
Radio (15 GHz)	2.00 ± 0.51	865	0.40	2.3×10^{-3}	3.4×10^{-2}
Optical	1.47 ± 0.08	957	0.51	9.7×10^{-2}	4.7×10^{-1}
<i>Swift</i> -UVOT	1.41 ± 0.12	806	0.46	5.6×10^{-3}	1.0×10^{-1}
<i>Swift</i> -XRT	1.50 ± 0.10	2521	0.47	1.4×10^{-1}	6.8×10^{-1}
<i>Fermi</i> -LAT	1.40 ± 0.26	786	0.40	2.0×10^{-5}	1.0×10^{-3}
MAGIC	1.00 ± 0.42	214	0.30	1.8×10^{-2}	3.7×10^{-1}

regime, consistent with a common synchrotron origin. Moreover, we found evidence for a correlation between the X-ray and VHE gamma-ray bands, as well as between the optical/UV/IR and HE gamma-ray bands. These findings support a scenario involving intertwined emission processes, such as those predicted by multi-zone synchrotron self-Compton (SSC) models [34].

Table 2: Results of the correlation study between integral fluxes in different bands, ordered by decreasing Spearman correlation coefficient. A simultaneity window of ± 1.5 days was assumed, extended to ± 10 days for correlations involving *Fermi*-LAT data. The p-values represent the significance of the null hypothesis (no correlation). Adapted from [27].

Band 1	Band 2	Spearman Coefficient	p-value
Optical	UV	0.94	4×10^{-88}
Optical	IR	0.90	2×10^{-50}
UV	HE γ -ray	0.66	3×10^{-10}
Optical	HE γ -ray	0.63	2×10^{-14}
UV	VHE γ -ray	0.62	9×10^{-8}
IR	HE γ -ray	0.61	1×10^{-5}
X-ray	VHE γ -ray	0.60	6×10^{-8}
IR	UV	0.60	4×10^{-6}
UV	X-ray	0.55	6×10^{-18}
Optical	X-ray	0.37	4×10^{-8}
HE γ -ray	VHE γ -ray	0.39	0.006
Optical	VHE γ -ray	0.35	2×10^{-5}
X-ray	HE γ -ray	0.32	0.006
IR	VHE γ -ray	0.26	0.09
IR	X-ray	0.29	0.02

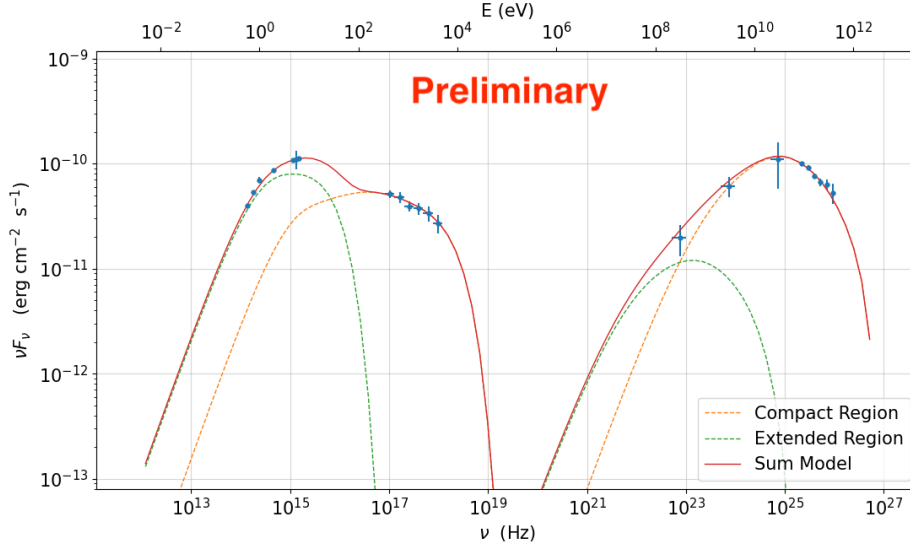


Figure 2: SED of PG 1553+113 from a flare of April 2019.

4. Modelling of the April 2019 flaring state

As anticipated from the 2.2-year modulation, the source entered a pronounced flaring episode in April 2019, reaching the highest VHE flux ever recorded for this object. Building on the results of MAGIC and multi-frequencies studies reported above, which indicated that single-zone models were insufficient to reproduce the full multiwavelength emission during high states, we applied—for the first time to this source—a two-zone synchrotron self-Compton (SSC) model.

The dataset was divided based on flux levels, revealing two distinct emission states: a high-activity state in April (flare) and a lower-activity state spanning June to August. To model the spectral energy distribution (SED), we employed the JetSet¹ open source framework, adopting two broken power-law electron distributions. Zone 1 accounts for the synchrotron and high-energy (HE) γ -ray emission, while Zone 2 reproduces the X-ray and very high energy (VHE) γ -ray components. Figure 2 shows the best model reproducing the flare data. The physical interpretation of the fitted parameters is still under investigation and will be the subject of a future publication.

5. Conclusions

Our multiwavelength study of PG 1553+113 over more than a decade confirms the presence of a strong ~ 2.2 -year periodicity in the gamma-ray and optical bands, while no significant periodic signal is detected at X-ray and TeV energies. The variability patterns and inter-band correlations support a multi-zone emission scenario. To interpret these observations, we have applied a two-zone synchrotron self-Compton model to the 2019 flare data, which successfully reproduces the spectral energy distribution and will provide insights into the source’s emission regions.

We emphasize that the physical interpretation of the model parameters is ongoing. In parallel, we are acquiring new observational data, particularly with IXPE, to further constrain the nature of

¹<https://github.com/andreatramacere/jetset>

the emission zones and the mechanisms driving the periodic variability. These efforts will help to refine our understanding of the complex processes at work in this intriguing blazar.

Acknowledgments

We would like to thank the Instituto de Astrofísica de Canarias for the excellent working conditions at the Observatorio del Roque de los Muchachos in La Palma. The financial support of the German BMBF, MPG and HGF; the Italian INFN and INAF; the Swiss National Fund SNF; the grants PID2019-107988GB-C22, PID2022-136828NB-C41, PID2022-137810NB-C22, PID2022-138172NB-C41, PID2022-138172NB-C42, PID2022-138172NB-C43, PID2022-139117NB-C41, PID2022-139117NB-C42, PID2022-139117NB-C43, PID2022-139117NB-C44, CNS2023-144504 funded by the Spanish MCIN/AEI/ 10.13039/501100011033 and "ERDF A way of making Europe; the Indian Department of Atomic Energy; the Japanese ICRR, the University of Tokyo, JSPS, and MEXT; the Bulgarian Ministry of Education and Science, National RI Roadmap Project DOI-400/18.12.2020 and the Academy of Finland grant nr. 320045 is gratefully acknowledged. This work was also been supported by Centros de Excelencia "Severo Ochoa" y Unidades "María de Maeztu" program of the Spanish MCIN/AEI/ 10.13039/501100011033 (CEX2019-000920-S, CEX2019-000918-M, CEX2021-001131-S) and by the CERCA institution and grants 2021SGR00426 and 2021SGR00773 of the Generalitat de Catalunya; by the Croatian Science Foundation (HrZZ) Project IP-2022-10-4595 and the University of Rijeka Project uniri-rirod-18-48; by the Deutsche Forschungsgemeinschaft (SFB1491) and by the Lamarr-Institute for Machine Learning and Artificial Intelligence; by the Polish Ministry Of Education and Science grant No. 2021/WK/08; and by the Brazilian MCTIC, CNPq and FAPERJ. EP acknowledges funding for the project "SKYNET: Deep Learning for Astroparticle Physics", 693 PRIN 2022 (CUP: D53D23002610006).

References

- [1] Hovatta T., Lindfors E., 2019, *New Astron. Rev.*, 87, 101541
- [2] Falomo R., Pian E., Treves A., 2014, *A&ARv*, 22, 73
- [3] Ulrich M.-H., Maraschi L., Urry C. M., 1997, *ARA&A*, 35, 445
- [4] Liodakis I., Romani R. W., Filippenko A. V., Kocevski D., Zheng W., 2019, *ApJ*, 880, 32
- [5] Raiteri C.M., et al., 2017b, *Nature*, 552, 374
- [6] Marscher A. P., 2016, *Galaxies*, 4, 37
- [7] Dorigo Jones J., et al., 2022, *MNRAS*, 509, 4330
- [8] Acciari V.A., et al., 2019, *MNRAS*, 486, 4233
- [9] Korochkin A., Neronov A., Semikoz D., 2020, *A&A*, 633, A74
- [10] Abramowski A., et al., 2015, *ApJ*, 802, 65
- [11] Aleksić J., et al., 2012, *ApJ*, 748, 46

- [12] Ackermann M., et al., 2015, ApJ, 813, L41
- [13] Abdollahi S., Baldini L., Barbiellini G., Bellazzini R., Berenji B., Bissaldi E., Blandford R. D., et al., 2024, ApJ, 976, 203
- [14] Covino S., Landoni M., Sandrinelli A., Treves A., 2020, ApJ, 895, 122
- [15] Peñil P., et al., 2020, ApJ, 896, 134
- [16] Romero G. E., Chajet L., Abraham Z., Fan J. H., 2000, A&A, 360, 57
- [17] Conway J. E., Murphy D. W., 1993, ApJ, 411, 89
- [18] Rieger F. M., 2004, ApJ, 615, L5
- [19] Honma F., Matsumoto R., Kato S., 1992, PASJ, 44, 529
- [20] Tchekhovskoy A., Narayan R., McKinney J. C., 2011b, MNRAS, 418, L79
- [21] Lehto H. J., Valtonen M. J., 1996, ApJ, 460, 207
- [22] Tavani M., Cavaliere A., Munar-Adrover P., Argan A., 2018, ApJ, 854, 11
- [23] Lico R., et al., 2020, A&A634, A87
- [24] Raiteri C.M. et al., 2017a, MNRAS, 466, 3762
- [25] Aleksić J., et al., 2015, MNRAS, 450, 4399
- [26] Guo J., Li H.-J., Bi X.-J., Lin S.-J., Yin P.-F., 2020, arXiv e-prints, p. arXiv:2002.07571
- [27] MAGIC Collaboration, et al., 2024, MNRAS, 529, 3894
- [28] Dhiman V., Gupta A. C., Gaur H., Wiita P. J., 2021, MNRAS, 506, 1198
- [29] Liodakis I., Romani R. W., Filippenko A. V., Kiehlmann S., Max-Moerbeck W., Readhead A. C. S., Zheng W., 2018, MNRAS, 480, 5517
- [30] O'Neill S., et al., 2022, ApJ, 926, L35
- [31] Sandrinelli A., Covino S., Treves A., Holgado A. M., Sesana A., Lindfors E., Ramazani V. F., 2018, A&A615, A118
- [32] Agarwal A., et al., 2021, A&A, 645, A137
- [33] Aniello T., Antonelli L. A., Tombesi F., Lamastra A., Middei R., Perri M., Saturni F. G., et al., 2024, A&A, 686, A300
- [34] MAGIC Collaboration, Abe K., Abe S., Abhir J., Abhishek A., Acciari V. A., Aguasca-Cabot A., et al., 2025, A&A, 695, A217